BIOCHEMISTRY
including biophysical chemistry & molecular biology
Article

Biochemistry **2010,** *49,* 2647–2656 2647
DOI: 10.1021/bi100022c

In Vitro Modulation of Cytochrome P450 Reductase Supported Indoleamine 2,3-Dioxygenase Activity by Allosteric Effectors Cytochrome b_5 and Methylene Blue

Josh T. Pearson,*,‡ Sophia Siu,§ David P. Meininger,§ Larry C. Wienkers,‡ and Dan A. Rock‡

‡*Biochemistry and Biophysics Group, Department of Pharmacokinetics and Drug Metabolism and* §*Department of Protein Sciences, Amgen Inc., 1201 Amgen Court West, Seattle, Washington 98119-3105*

Received November 20, 2009; Revised Manuscript Received February 23, 2010

ABSTRACT: Indoleamine 2,3-dioxygenase (IDO) is a heme-containing dioxygenase involved in the degradation of several indoleamine derivatives and has been indicated as an immunosuppressive. IDO is an attractive target for therapeutic intervention in diseases which are known to capitalize on immune suppression, including cancer, HIV, and inflammatory diseases. Conventionally, IDO activity is measured through chemical reduction by the addition of ascorbate and methylene blue. Identification of potential coenzymes involved in the reduction of IDO in vivo should improve in vitro reconstitution systems used to identify potential IDO inhibitors. In this study we show that NADPH−cytochrome P450 reductase (CPR) is capable of supporting IDO activity in vitro and that oxidation of L-Trp follows substrate inhibition kinetics ($k_{cat} = 0.89 \pm 0.04\ s^{-1}$, $K_m = 0.72 \pm 0.15\ \mu M$, and $K_i = 9.4 \pm 2.0\ \mu M$). Addition of cytochrome b_5 to CPR-supported L-Trp incubations results in modulation from substrate inhibition to sigmoidal kinetics ($k_{cat} = 1.7 \pm 0.3\ s^{-1}$, $K_m = 1.5 \pm 0.9\ \mu M$, and $K_i = 1.9 \pm 0.3$). CPR-supported D-Trp oxidations (±cytochrome b_5) exhibit Michaelis−Menten kinetics. Addition of methylene blue (minus ascorbate) to CPR-supported reactions resulted in inhibition of D-Trp turnover and modulation of L-Trp kinetics from allosteric to Michaelis−Menten with a concurrent decrease in substrate affinity for IDO. Our data indicate that CPR is capable of supporting IDO activity in vitro and oxidation of tryptophan by IDO displays substrate stereochemistry dependent atypical kinetics which can be modulated by the addition of cytochrome b_5.

Indoleamine 2,3-dioxygenase (IDO)[1] is a heme-containing dioxygenase responsible for the oxidative cleavage of several indoleamine derivatives (*1*−*3*), including the initial and rate-limiting step of tryptophan degradation along the kynurenine pathway (*4*). IDO is widely expressed in a variety of cell types including macrophages, eosinophils, dendritic cells, B cells, endothelial cells, and various types of tumor cells (*5*−*10*), with IDO gene expression regulated by various cytokines, most importantly by interferon-γ (IFNγ) (*11*, *12*). IDO has been implicated as an immunosupporessive, contributing to maternal tolerance toward the allogeneic fetus (*13*), suppression of transplant rejection (*14*, *15*), and regulation of autoimmune disorders (*16*−*18*), with its expression in cancer cells correlating with poor prognosis (*19*, *20*).

Heme-containing proteins represent a vital class of enzymes often involved in physiological homeostasis, whereupon their activity can be modulated by their electron transfer partners (*21*−*23*). Moreover, heme protein activity is impacted by the ring structure used to sequester the iron (heme form) and the subsequent protein folding environment used to bind the heme. In combination, the two structural features create the active protein (holoenzyme), whereby the binding of various cofactors, electron transfer partners, and/or ligands can impact electron transfer and modulate catalytic activity in order to control the extent of biochemical response (*24*). Therefore, prior to targeting a heme protein for disease modification it is imperative to develop a basic understanding of a heme protein's sensitivity toward different reducing systems. Such efforts can provide assurance that the reconstituted in vitro enzyme activity represents the activity under physiological conditions.

For IDO, the endogenous cofactor has yet to be identified. Recently, Maghzal et al. reported cytochrome b_5 is capable of reducing Fe^{3+}-IDO to support catalytic activity (*25*). In this study, the authors showed direct reduction of IDO by cytochrome b_5 in a system containing NADPH−cytochrome P450 reductase (CPR) and a NADPH regenerating system. Activity assays with increasing concentrations of cytochrome b_5 resulted in an increase in kynurenine formation, and knock down of cytochrome b_5 protein expression in HEK 293 cells by siRNA resulted in decreased IDO activity. At 400 μM L-Trp, CPR alone showed no activity but was a requirement for cytochrome b_5 reduction of Fe^{3+}-IDO and enzymatic activity. Although indirectly, Vottero and co-workers were the first to observe a potential role for cytochrome b_5 as an electron transfer coenzyme to IDO by the use of a tryptophan auxotroph yeast strain transduced with human IDO (*26*). Their data showed that decreased levels of cytochrome b_5 led to an increase in cell growth, which was interpreted to be due to lower activation of IDO and therefore inhibition of Trp catabolism.

*Corresponding author. Telephone: (206) 265-7823. Fax: (206) 217-0492. E-mail: joshuap@amgen.com.

[1]Abbreviations: IDO, indoleamine 2,3-dioxygenase; L-Trp, L-tryptophan; D-Trp, D-tryptophan; CPR, NADPH−cytochrome P450 reductase (alternatively named P450 oxidoreductase); b_5, cytochrome b_5; MethBlue, methylene blue; PBS, phosphate-buffered saline; P450, cytochrome P450; CHAPS, 3-[(3-cholamidopropyl)dimethylammonio]-1-propanesulfonate; TCA, trichloroacetic acid; NADPH, β-nicotinamide adenine dinucleotide 2′-phosphate reduced tetrasodium salt hydrate; 1-L-MT, 1-L-methyl-Trp; DOPC, 1,2-dioleoyl-*sn*-glycero-3-phosphocholine; DLPS, 1,2-dilauroyl-*sn*-glycero-3-phospho-L-serine; DLPC, 1,2-dilauroyl-*sn*-glycero-3-phosphocholine; kan, kanamycin; TB, terrific broth.

Published on Web 02/23/2010

The discovery of a potential in vivo electron transfer partner capable of reducing IDO and supporting activity is fundamental to furthering our understanding of IDO biochemistry and elucidating inhibitors to modulate its activity in vivo. To date, kinetic characterization of purified human IDO has been conducted through the use of a chemical reducing system that consists of ascorbate and methylene blue (*1*). The use of chemical reducing systems can provide insight into the potential catalytic rate and efficiency of IDO, but the data acquired may misrepresent or conceal key ligand−enzyme interactions masking the ability to understand ligand structure function relationships. For example, interactions with electron transfer partners may lead to conformational changes that alter kinetics or affinities of the enzyme for its substrate(s), inhibitor(s), cofactors, or even additional electron transfer partners.

CPR is the endogenous electron transfer partner for the cytochrome P450 family of enzymes, transferring the obligate two electrons from NADPH individually to the P450 at two separate steps in the catalytic cycle (*27*). Cytochrome b_5 has been shown to stimulate P450 activity for various isoforms, either through transfer of the second electron (from either CPR or NADH cytochrome b_5) (*21*, *22*, *28*) to P450 or through an allosteric effect resulting in more efficient catalysis (*23*, *29*−*31*). Multiple ligand binding, homotropic or heterotropic, can also induce an allosteric effect, resulting in atypical kinetics for P450 enzymes (*32*−*36*). Sono showed similar results for IDO, whereupon binding of an effector increased the affinities for the substrates L- and D-Trp and led to substrate/effector-dependent changes in reaction kinetics (*37*). Substrate inhibition kinetics for L-Trp has also been observed for rabbit IDO (*1*, *38*). Lu et al. recently expanded upon these observations showing substrate inhibition kinetics for L-Trp with recombinant human IDO and modulation of these kinetics by the effector 3-indole ethanol (*39*).

Even though evolutionarily distinct, the similarity to cytochrome P450 enzymes in regard to effector binding, atypical kinetics, and the potential interactions with b_5 (*25*, *26*) led us to further investigate the potential roles CPR and cytochrome b_5 play in modulating IDO enzymology. The present study reveals that CPR alone is capable of supporting IDO enzymatic activity and that IDO can be modulated differentially by the addition of the coenzyme cytochrome b_5 or the ligand methylene blue.

MATERIALS AND METHODS

Materials. L-kynurenine, L- and D-Trp, 1-L-methyl-Trp, formic acid, 3-NO-tyrosine, methylene blue, trichloroacetic acid, acetonitrile, and ascorbic acid were of the highest grade available from Sigma-Aldrich (St. Louis, MO). Reduced β-NADPH was purchased from EMD Chemicals, Inc. (Gibbstown, NJ), and DOPC, DLPC, and DLPS were purchased from Avanti Polar Lipids, Inc. (Alabaster, AL). Purified recombinant human cytochrome b_5 was purchased from Invitrogen, and purified recombinant human cytochrome P450 reductase was purchased from BD Gentest.

Protein Expression and Purification. Residues 2−403 of human IDO were fused to an N-terminal hexahistidine (His(6) tag via PCR. *Escherichia coli* strain BL21 Star (Stratagene) was transformed with pAMG21 His(6)-IDO for expression of soluble enzyme. Transformed colonies selected on agarose plates containing 50 μg/mL kanamycin (kan) were used to generate small starter cultures in TB media with 50 μg/mL kan at 37 °C. Starter cultures were scaled up to 1 L in TB/kan media supplemented with 500 μM δ-aminolevulinic acid (ALA). Soluble His(6)-IDO expression was induced via addition of 0.5 ng/mL *N*-(β-ketocaproyl)-DL-homoserine lactone (Sigma) at cell densities of ∼0.5 OD at 600 nm. Overnight induction at 18 °C produced purified protein lots of higher specific activity than those induced for shorter periods of time or at higher temperatures. Final cell densities of 12−13 OD at 600 nm were typical for successful productions.

Cells were harvested by centrifugation at 5000*g* for 30 min at 4 °C. Cell pellets were homogenized in lysis buffer and passed through a Microfluids model 110 L microfluidizer operating at 16000 psi nitrogen gas with the lysis cell and lysate receptacle chilled on ice. Lysates were clarified via centrifugation at 4 °C for 45 min at 28000*g* prior to purification.

IDO lysis buffer consisted of 25 mM Tris, 20 mM imidazole, pH 7.4, and 150 mM NaCl supplemented with EDTA-free Complete protease inhibitor (Roche) and benzonase nuclease HC (Novagen). Clarified cell lysate from 1 L of culture volume was sterile filtered and loaded onto a 5 mL HisTrap FF (GE Healthcare) column, preequilibrated in 25 mM Tris, pH 7.4, 20 mM imidazole, and 300 mM NaCl. The column was washed with 25 mM Tris, 40 mM imidazole, pH 7.4, and 300 mM NaCl and protein eluted with a 5 column volume linear gradient from 40 to 250 mM imidazole in 25 mM Tris, pH 7.4, and 300 mM NaCl. Elution fractions containing human IDO were further purified by preparative size exclusion chromatography (SEC) on a HiLoad 26/60 Superdex 200 column (GE Healthcare) with a mobile phase consisting of 50 mM Tris, pH 7.4, and 1 mM EDTA. All purification steps were carried out at 4 °C on an Akta Express chromatography system (GE Healthcare). SEC aliquots were pooled based on relative His(6)-IDO content as assessed by SDS−PAGE, flash-frozen in liquid nitrogen, and stored at −80 °C. Purified protein was >95% pure as assessed by analytical SEC with an A_{406}/A_{280} ratio of 1.65.

LC-MS/MS Quantitation of Analytes. All quantitative measurements were conducted on a 4000 Q-Trap from Applied Biosystems (San Jose, CA) connected to a Shimadzu HPLC including a degasser. A sample volume of 20 μL was injected onto a Waters YMC ODS-AQ column (2.0 × 50 mm) at a flow rate of 250 μL/min. Initial HPLC conditions were 100% solvent A (2.0% formic acid in water). The elution gradient increased from 0% to 35% B (0.1% formic acid in acetonitrile) in 2 min, 35−90% B in 0.2 min, and was held at 90% B for 0.5 min before equilibration back to initial conditions. Quantitation of kynurenine was conducted by using the MRM function monitored by a Q1 set at m/z 209.07 and Q3 at m/z 146.40, with the declustering potential at 41 and a collision energy of 25 (arbitrary units). Trp levels were monitored by a Q1 m/z of 205.05 and Q3 188.10, with a declustering potential of 55 and a collision energy of 17. For quantitation, an internal standard, 3-NO-tyrosine, was monitored by a Q1 set at m/z 227.09 and a Q3 m/z of 181.0, with the declustering potential at 36 and a collision energy of 21. Mass spectral settings common to all analytes were the dwell time, 250 ms; curtain gas, 10; IonSpray gas 1 and 2 set at 40; IonSpray voltage, 4500; and the source temperature at 450 °C.

Reconstitution of Purified Human Cytochrome CPR and Human Cytochrome b_5. Reconstitutions of purified CPR and purified cytochrome b_5 were conducted as originally described by Shaw et al. (*40*). Briefly, purified CPR or purified CPR mixed with purified cytochrome b_5 was placed on ice for 5 min. A 1:1:1 mixture of the lipids, DOPC, DLPC, and DLPS, at a total lipid concentration of 1 mg/mL was added to yield a final 0.1 mg/mL

concentration after dilution and allowed to sit on ice for an additional 5 min. Following 5 min equilibration, CHAPS (5 mg/mL) was then added to yield a final concentration of 0.5 mg/mL after dilution and allowed to sit on ice for 5 min. Samples were then diluted with PBS and used as cofactor working stocks.

IDO Enzymatic Activity Assays. IDO activity was assessed by measuring the formation of kynurenine from either L- or D-Trp versus time. Purified human IDO was diluted into PBS (pH 7.4) containing either 20 mM ascorbate (brought to pH 7.4 by addition of NaOH) or reconstituted CPR (±cytochrome b_5) working stock and divided into 800 μL aliquots. Substrate at varying concentrations, dissolved in 1:2 DMSO to water, was diluted 100-fold into each respective aliquot, mixed by pipet, and plated into eight 90 μL aliquots. Plates were preincubated at 37 °C for 5 min before initiation of reaction with 10 μL of either 100 μM methylene blue (ascorbate incubations), 10 mM NADPH (CPR cofactor supported incubations), or PBS for negative control (four of the eight replicates). Individual incubations (100 μL) contained a final 0.2 pmol of IDO. Incubations were allowed to proceed for 2 min at 37 °C with shaking before being quenched by the addition of 200 μL of 10% TCA in water containing 2 μM 3-NO-tryosine as the internal standard. Plates were heat sealed and placed at 60 °C for 1 h (*41*), centrifuged, and then analyzed by LC-MS/MS. Standard curves of L-kynurenine were prepared fresh each day and treated under the same conditions as incubation samples. Negative control samples were analyzed for kynurenine impurities at each substrate concentration studied, averaged, and subtracted from the measured activities.

IC_{50} Determination. The incubation time and protein concentrations used were within the linear range for each respective cofactor system. In addition, no more than 15−20% turnover of L-Trp occurred over the 2 min incubation time. L-Trp was run at a concentration of 2 μM for the three cofactor systems, and all incubations contained less than 1% organic solvent (v/v; acetonitrile). Incubation conditions (run in triplicate) were identical to those listed above for enzymatic activity assays.

K_i Determination. A matrix of six probe substrate concentrations (5, 10, 20, 25, 50, and 150 μM D-Trp) and six inhibitor concentrations (0, 0.01, 0.1, 1, 10, and 100 μM) was used to determine a K_i value. Reaction conditions and sample preparation procedures were identical to those described above for the IC_{50} determinations. All K_i determinations were run in triplicate.

Statistical Analysis. Standard curves and mass spectrometry data were fit using Analyst (version 1.4; Applied Biosystems, Foster City, CA). Standard curves were weighted using $1/x$ unless stated otherwise. Analysis of kinetic and inhibition constant data was performed using GraphPad Prism (version 5.00; GraphPad Software Inc., San Diego, CA). Enzyme kinetic data were fit to each of three models, either Michaelis−Menten, substrate inhibition (eq 1)

$$v = V_{max}[S]/(K_m + [S](1 + [S]/K_i)) \quad (1)$$

or allosteric sigmoidal (eq 2)

$$v = V_{max}[S]^n/(K' + [S]^n) \quad (2)$$

and compared by statistical analysis and visual inspection through the use of reciprocal plots. For the Hill equation (e.g., eq 2), K' is a constant comprising the interaction factors and no longer equals K_m except when n is equal to 1 (*42*). For reported k_{cat} values, measured product concentrations were corrected for time and protein concentration prior to determination of V_{max} values. IC_{50} data were fit using a sigmoidal dose−response model (eq 3).

$$\%\ \text{remaining activity} = \text{min} + (\text{max} - \text{min})/(1 + 10\text{^}(\log [I] - \log IC_{50})) \quad (3)$$

After visual inspection of the Lineweaver−Burk plots, K_i data were fit globally to the appropriate model and evaluated against the other two potential models. Data were fit globally to the mixed-inhibition model (eq 4), competitive (eq 5), or noncompetitive (eq 6).

$$v = (V_{max}/(1 + [I]/\alpha K_i))[S]/((K_m(1 + [I]/K_i)/(1 + [I]/\alpha K_i)) + [S]) \quad (4)$$

$$v = V_{max}[S]/((K_m(1 + [I]/K_i)) + [S]) \quad (5)$$

$$v = (V_{max}/(1 + [I]/K_i))[S]/(K_m + [S]) \quad (6)$$

Definition of terms for the above equations are [I] is the concentration of inhibitor in the system, [S] is the concentration of substrate, K_m is equal to the substrate concentration at half the maximal reaction velocity, V_{max} is equal to the maximal velocity, K_i is the dissociation constant for the enzyme−inhibitor complex, α describes the mechanism of inhibition, and n is the Hill coefficient.

Active Site Modeling. The crystallography coordinates of IDO were used from 2D0T.pdb (*43*). The resolution of this ligand-bound structure was at 2.3 Å. The pdb coordinates were input into Maestro (Schrodinger, NY). The protein structure was prepared using protein preparation script which steps through structural optimization of protein structure followed by minimization. Briefly, the initial structure was preprocessed and analyzed for correct bond order, overlapping residues, added any missing hydrogens, and removed water molecules beyond 5 Å. Heteroatom ionization states were for the heme iron followed by hydrogen bond optimization. The resulting structure was minimized using an OLPS2005 force field to an rmsd of 0.3 Å. SiteMap (Schrodinger, NY) was used to identify α sites (active binding sites) on IDO. The SiteMap defined active site was used to generate a docking grid for Glide docking of L-Trp. The final structure was minimized. SiteMap was reexamined using the new L-Trp-bound structure as described above.

RESULTS

CPR-Supported IDO Activity. The activity of purified human IDO was examined with the addition of varying concentrations of reconstituted human CPR (0.7−75 nM). Incubations utilizing L-Trp as the substrate (0−20 μM) display substrate inhibition kinetics (Figure 1A; Supporting Information Table 1) with increasing levels of CPR increasing k_{cat} but having no effect on K_m or K_i. The fitted parameters from eq 1 for K_m and K_i are 0.72 ± 0.15 and 9.4 ± 2.0 μM, respectively. The k_{cat} values range from 0.29 ± 0.02 to 0.67 ± 0.06 s^{-1} for incubations with 0.7 to 75 nM CPR, respectively. Incubations with D-Trp (0−300 μM) display Michaelis−Menten kinetics (Figure 1B; Supporting Information Table 1) with a K_m value of 25.4 ± 3.2 μM and k_{cat} values that range from 0.36 ± 0.01 to 0.68 ± 0.03 s^{-1} for incubations with 0.7 and 75 nM CPR, respectively. IDO activity as a function of CPR concentration (0−500 nM) in the presence of saturating D-Trp (300 μM) yields an "effective" K_m for CPR of

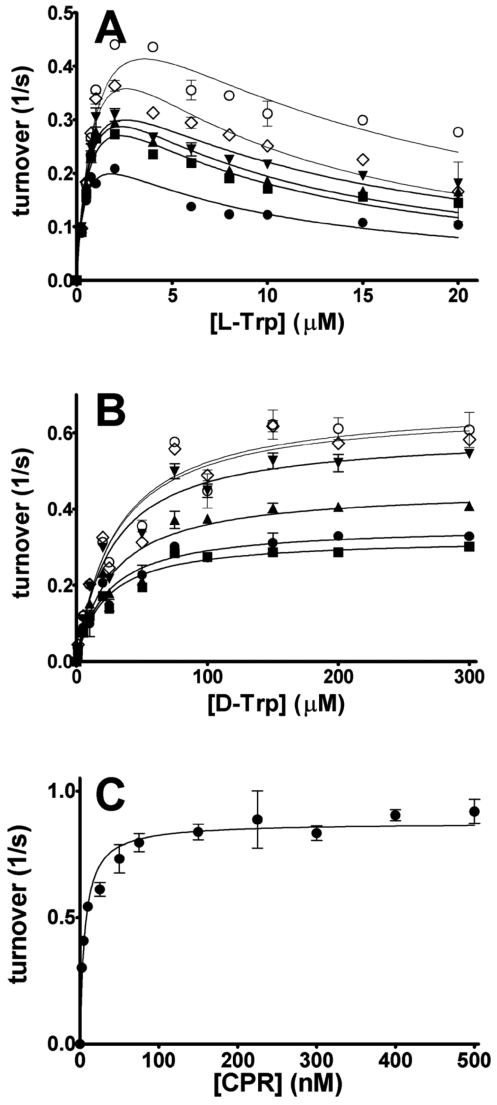

FIGURE 1: CPR-supported IDO activity. (A) Kinetic traces displaying substrate inhibition for L-Trp oxidation by CPR-supported IDO activity. CPR concentrations were 0.7 (●), 2.2 (■), 4.5 (▲), 20 (▼), 37.5 (◇), and 75 nM (○). (B) Michaelis−Menten kinetics for CPR-supported IDO utilizing D-Trp as substrate. CPR concentrations were matched to (A). (C) Plot of enzyme activity for D-Trp (300 μM) versus CPR concentration.

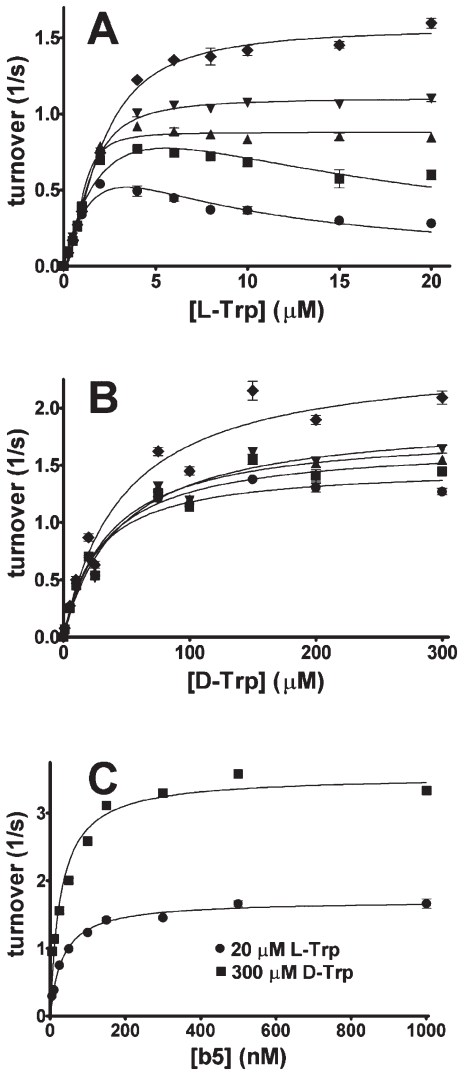

FIGURE 2: Cytochrome b_5 dependent modulation of IDO activity. (A) Modulation of CPR- (200 nM) supported L-Trp oxidation kinetics with increasing concentrations of cytochrome b_5. Concentrations of cytochrome b_5 utilized were 0.0 (●), 6.6 (■), 13 (▲), 33 (▼), and 66 (◆). (B) D-Trp oxidation kinetics with increasing amounts of cytochrome b_5. (C) Plot of enzyme activity for L-Trp (20 μM) and D-Trp (300 μM) versus cytochrome b_5 concentration.

6.0 ± 0.6 nM (Figure 1C) and maximal k_{cat} value of 0.87 ± 0.01 s^{-1}. Subsequent experiments utilized saturating concentrations of CPR (200 nM) with varying amounts of cytochrome b_5. At 200 nM CPR, L-Trp catabolism by IDO has a maximal k_{cat} value of 0.89 ± 0.04 s^{-1} (Supporting Information Table 1).

Cytochrome b_5 Modulation of Substrate Inhibition Kinetics. At 6.6 nM cytochrome b_5, L-Trp (0−20 μM) oxidation continues to display substrate inhibition kinetics but with an increase in the K_i to 15.6 ± 1.9 μM (Figure 2A; Supporting Information Table 2). No significant changes in K_m or k_{cat} are observed compared to activities measured in the absence of cytochrome b_5. However, as cytochrome b_5 concentrations increase from 13 to 400 nM, the kinetic behavior of L-Trp changes significantly. At high concentrations of cytochrome b_5 the kinetics display sigmoidal behavior, with K_m and n (Hill coefficient) values of 1.5 ± 0.9 μM and 1.9 ± 0.3, respectively. The oxidation of D-Trp with increasing concentrations of cytochrome b_5 continued to display Michaelis−Menten kinetics but results in an increase in K_m and k_{cat}, with K_m increasing ~1.7-fold to 45.9 ± 1.3 μM in the presence of cytochrome b_5 concentrations ranging from 33 to 400 nM (Figure 2B; Supporting Information Table 2). IDO activity as a function of cytochrome b_5 concentration (5−1000 nM) in the presence of saturating concentrations of L-Trp (20 μM) and D-Trp (300 μM) yield "effective" K_m values for cytochrome b_5 of 33.4 ± 2.4 μM (L-Trp) and 28.0 ± 2.7 μM (D-Trp) with maximal k_{cat} values for L-Trp and D-Trp of 1.7 ± 0.3 and 3.5 ± 0.1 s^{-1}, respectively (Figure 2C).

Methylene Blue-Supported Tryptophan Oxidation. Ascorbate/methylene blue-supported oxidation of L-Trp (0−200 μM) displays substrate inhibition kinetics with a K_m of 3.1 ± 0.3 μM, a K_i of 225 ± 36 μM, and a k_{cat} of 0.99 ± 0.4 s^{-1} (Supporting Information Figure 1A). D-Trp (0−10 mM) with ascorbate/methylene blue-supported activity follows Michaelis−Menten kinetics with a K_m of 1.03 ± 0.23 mM and k_{cat} of 1.7 ± 0.1 s^{-1} (Supporting Information Figure 1B). Experiments conducted which employ an extended concentration range of L-Trp (0−200 μM) in CPR-supported incubations display partial substrate inhibition, i.e., never reaching complete inhibition of activity (Figure 3). Addition of 250 nM cytochrome b_5 to this

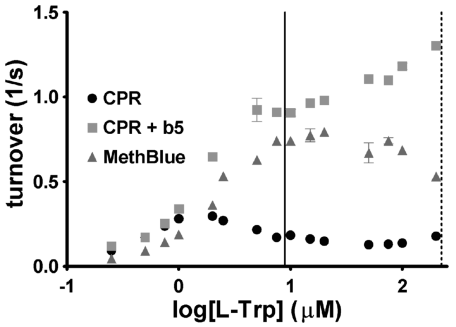

FIGURE 3: Methylene blue-supported tryptophan oxidation. Plot of IDO activity versus log L-Trp concentration showing partial substrate inhibition of CPR-supported incubations. Addition of 250 nM cytochrome b_5 abolishes the observed substrate inhibition. Methylene blue-supported reactions also observe substrate inhibition but with a lower affinity K_i. Added lines represent the K_i values for CPR- (solid line) and methylene blue- (dashed line) supported L-Trp oxidation reactions.

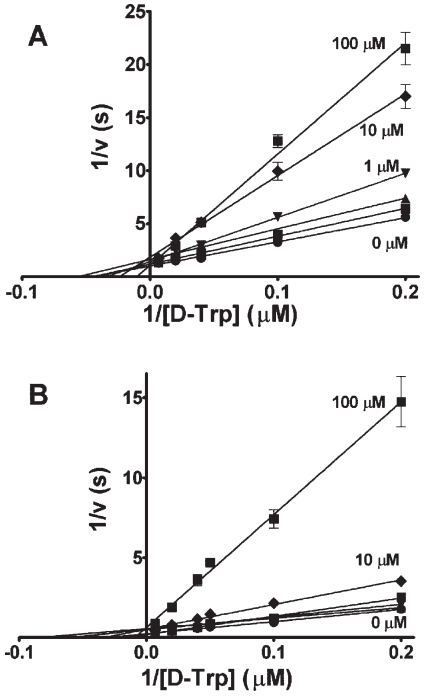

FIGURE 4: Inhibition of CPR-supported D-Trp oxidation by methylene blue. Lineweaver−Burk plots for visual inspection of methylene blue-dependent inhibition of D-Trp oxidation in CPR- (A) and CPR plus cytochrome b_5- (B) supported reactions. Concentrations of CPR and cytochrome b_5 were 200 and 250 nM, respectively.

system abolishes the observed partial substrate inhibition for L-Trp but continues to display nonlinear, or atypical, kinetics. Methylene blue-supported L-Trp oxidation also displays substrate inhibition kinetics, although with a higher K_i, which renders the distinction between complete or partial substrate inhibition indiscernible.

Methylene Blue Inhibition of CPR-Supported D-Trp Oxidation. Addition of methylene blue (0−100 μM) to CPR-supported D-Trp incubations (±cytochrome b_5) leads to concentration-dependent inhibition of IDO activity (Figure 4). For incubations minus cytochrome b_5, i.e., CPR alone, the data are best described by a competitive inhibition model, with a K_i value of 57.2 ± 13.6 μM. For CPR plus cytochrome b_5, methylene blue inhibition of D-Trp oxidation followed a mixed mode of inhibition (*44*), with a K_i of 9.0 ± 1.9 μM and an α value of 3.6 ± 2.2.

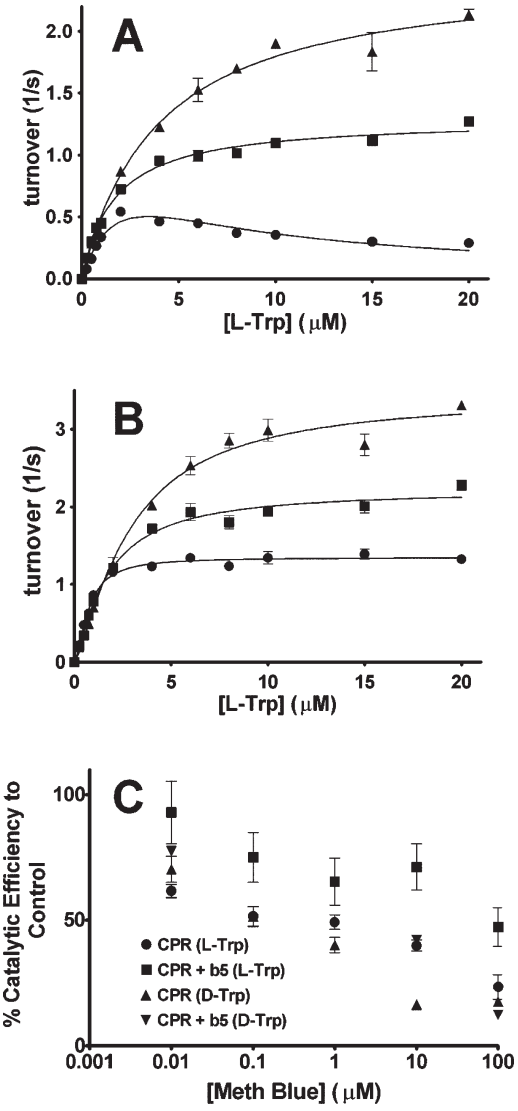

FIGURE 5: Methylene blue-dependent modulation of CPR-supported L-Trp oxidation. (A) Modulation of CPR- (200 nM) supported L-Trp oxidation kinetics with increasing concentrations of methylene blue: 0.0 (●), 0.1 (■), and 0.5 μM (▲). (B) Addition of methylene blue to CPR- (200 nm) plus cytochrome b_5- (250 nM) supported reactions continues to display allosteric sigmoidal kinetics with increasing amounts of methylene blue up to 1 μM, but with a concomitant decrease in the Hill coefficient. At 10 μM L-Trp reactions display Michaelis−Menten kinetics with, by definition, a Hill coefficient of 1 (see Table 1). (C) Plot of percent catalytic efficiency (k_{cat}/K_m) from kinetic constants normalized to 0 μM methylene blue (control) for CPR- (200 nM) and CPR (200 nM) with cytochrome b_5- (250 nM) supported incubations of L- and D-Trp. Addition of methylene blue (minus ascorbate) leads to a concentration-dependent loss in catalytic efficiency.

Methylene Blue Modulation of CPR-Supported L-Trp Oxidation. Addition of methylene blue (0−30 μM) to CPR-supported L-Trp oxidation reactions results in a switch from substrate inhibition kinetics to Michaelis−Menten with increasing methylene blue concentration decreasing the affinity of IDO for L-Trp (Figure 5A and Table 1). CPR plus cytochrome b_5-supported L-Trp oxidation reactions continue to display sigmoidal kinetics upon the addition of methylene blue up to a concentration of 1 μM (Figure 5B) but result in a methylene blue concentration-dependent decrease in affinity for the substrate L-Trp and the Hill coefficient (n value). At 10 and 30 μM methylene blue, a decrease in the affinity for L-Trp continues to

Table 1: Kinetic Constants Determined for CPR-Supported L-Trp Oxidation in the Presence of Methylene Blue[a]

MethBlue (μM)	[b_5] (nM)	kinetic model	K_m[b] (μM)	k_{cat} (1/s)	K_{cat}/K_m ($s^{-1}\mu M^{-1}$)	K_i (μM)	n (Hill coeff)
0.0	0	SI[c]	0.72 ± 0.15	0.87 ± 0.01	1.2 ± 0.4	9.4 ± 2.0	N/A[d]
0.1	0	M-M	1.7 ± 0.1	1.3 ± 0.1	0.76 ± 0.05	N/A	N/A
0.5	0	M-M	3.9 ± 0.4	2.5 ± 0.1	0.64 ± 0.06	N/A	N/A
1.0	0	M-M	4.9 ± 0.4	3.0 ± 0.1	0.61 ± 0.05	N/A	N/A
10	0	M-M	12.9 ± 1.0	6.4 ± 0.3	0.49 ± 0.04	N/A	N/A
30	0	M-M	27.9 ± 8.0	8.1 ± 1.6	0.29 ± 0.08	N/A	N/A
0.0	250	AS	1.5 ± 0.9	1.7 ± 0.3	1.1 ± 0.71	N/A	1.9 ± 0.3
0.1	250	AS	1.9 ± 0.2	2.2 ± 0.1	1.0 ± 0.21	N/A	1.3 ± 0.1
0.5	250	AS	4.0 ± 0.4	3.4 ± 0.1	0.85 ± 0.17	N/A	1.3 ± 0.1
1.0	250	AS	5.4 ± 0.7	4.2 ± 0.2	0.74 ± 0.16	N/A	1.2 ± 0.1
10	250	M-M	12.4 ± 1.1	10.0 ± 0.5	0.80 ± 0.16	N/A	1.1 ± 0.1[e]
30	250	M-M	22.4 ± 3.9	12.0 ± 1.5	0.54 ± 0.13	N/A	0.9 ± 0.1[e]

[a]CPR concentration equal to 200 nM. [b]Kinetic traces fit to the allosteric sigmoidal model (Hill equation) report K' values where K' comprises the interaction factors for the n sites of substrate binding. [c]Kinetic model abbreviations: SI, substrate inhibition; M-M, Michaelis−Menten; AS, allosteric sigmoidal. [d]N/A, not applicable. [e]Determined from fit to AS model; by statistical criteria the data were better represented by the Michaelis−Menten equation which is equivalent to a Hill coefficient of 1.

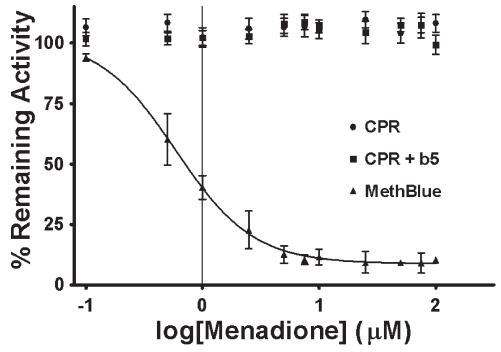

FIGURE 6: Reduction system dependent differences in menadione IC_{50} values. Plot of the percent remaining activity for the oxidation of L-Trp by IDO versus the log concentration of menadione when utilizing our three different reducing systems, CPR (200 nM), CPR (200 nM) + b_5 (250 nM), and ascorbate/methylene blue.

be observed in parallel with increasing concentrations of methylene blue, with the Hill coefficient reaching a value of 1 and resulting in Michaelis−Menten kinetics (Table 1). Figure 5C shows the concentration-dependent changes in catalytic efficiency (k_{cat}/K_m) for CPR-supported L- and D-Trp oxidation with increasing methylene blue concentrations.

Cofactor-Dependent Inhibition of L-Trp Oxidation by Menadione. Incubations of L-Trp (at the corresponding K_m values) and IDO with varying concentrations of menadione result in differential inhibition. With reactions supported by CPR, menadione failed to inhibit L-Trp regardless of the presence or absence of cytochrome b_5 in the incubation (Figure 6). Conversely, menadione was shown to effectively inhibit L-Trp oxidation from reactions supported with ascorbate/methylene blue, yielding an IC_{50} value of 0.64 ± 0.08 μM, similar to the previously reported value of 1.0 μM (*41*).

Model of Potential Effector Binding Site Adjacent to Active Site. The principal active site was identified above the heme using SiteMap as described in the Materials and Methods section (Figure 7A). Subsequent docking of L-Trp was performed to generate a new ligand bound structure. The new ligand-bound model was subjected to SiteMap to identify a potential allosteric binding site from the newly formed complex (Figure 7B). The primary α site identified from the complex overlaps with the original binding site but also occupies additional space adjacent to the heme and near bulk solvent. The new pocket from L-Trp-bound IDO (Figure 7C) accounts for the volume displaced by L-Trp as evidenced by the similar α site volumes of 332 Å^3 compared to 308 Å^3 for L-Trp versus the apo structure, respectively. This newly formed α site presents a novel site for cofactor interaction.

DISCUSSION

IDO is an attractive target for therapeutic intervention in diseases which are known to capitalize on immune suppression including cancer, HIV, and inflammatory diseases. Despite the established role of IDO in immune suppression, only one clinical candidate has been evaluated to date, 1-D-methyltryptophan (D-1MT), a weak inhibitor of IDO (Figure 8). The natural product annulin B and menadione represent a structurally distinct class of inhibitors from D-1MT, and both compounds have been shown to inhibit IDO in vitro (*41*, *45*). The inhibitors shown in Figure 8 demonstrate the flexibility of IDO to bind different chemical motifs, e.g., the indole of Trp to the naphthoquinoline moiety of annulin B, which possess unique physiochemical properties and spatially distinct pharmacophores. Moreover, the redox activities of menadione may contribute to the mechanism by which it inhibits IDO. The presence or absence of different enzyme cofactors and/or electron transfer partners may impact the dynamics of the active site. The sensitivity of IDO toward different effectors, in combination with the limited knowledge regarding its endogenous electron transfer partners or cofactors essential for oxidative activity, requires further attention to understanding the biochemistry of IDO.

Conventionally, IDO is reconstituted with methylene blue and ascorbic acid to achieve oxidative activity toward Trp. The artificial nature of this reconstitution system has the potential to mask or alter the biochemical characteristics of the enzyme. Here we show that reconstitution of recombinant purified CPR into lipids according to the protocol published by Shaw (*40*), followed by dilution into IDO reaction mixture (PBS, IDO protein, and substrate), results in NADPH-dependent formation of *N*-formylkynurenine, which is subsequently converted to kynurenine through acidification. With D-Trp as the substrate, IDO follows Michaelis−Menten kinetics (Figure 1B, Supporting Information Table 1) but observes substrate inhibition kinetics with its endogenous substrate L-Trp (Figure 1A, Supporting Information Table 1). Varying the concentration of CPR per incubation leads to an increase in k_{cat} with no change in the kinetic behavior observed for either substrate, L- or D-Trp

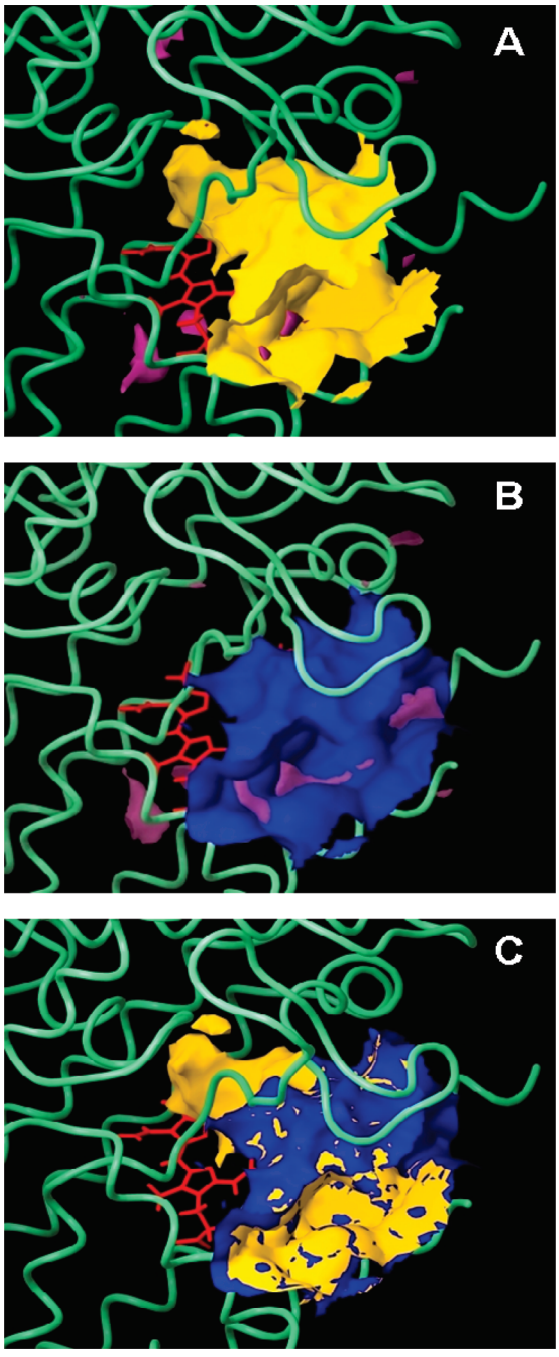

FIGURE 7: Active site map of Apo IDO and L-Trp-bound IDO. (A) Mapped surface area of the primary α site identified from Apo IDO structure from 2D0T.pdb. The surface area was calculated to be 1038 Å^3. The hydrophobic surface contact points are highlighted in purple. The relative hydrophobic/hydrophilic contact area of the α site was 0.67. (B) Mapped surface area of the primary α site identified from IDO with L-Trp docked within the active site. The hydrophobic surface contact points are highlighted in purple. The relative hydrophobic/hydrophilic contact area of the α site was 0.57. (C) Comparison of the α sites from the Apo vs L-Trp-docked models show a large degree of overlap. The α site from the bound structure displaces accessible volume distal to the heme where L-Trp docks but adds additional volume adjacent to heme with additional area for hydrophobic contact.

(Figure 1A,B). A plot of CPR concentration versus reaction velocity at a saturating concentration of D-Trp (300 μM) follows Michaelis−Menten kinetics with a K_m of electron transfer from CPR to IDO equal to 6.0 ± 0.6 nM and a maximal reaction velocity for the IDO dependent oxidation of D-Trp at saturating

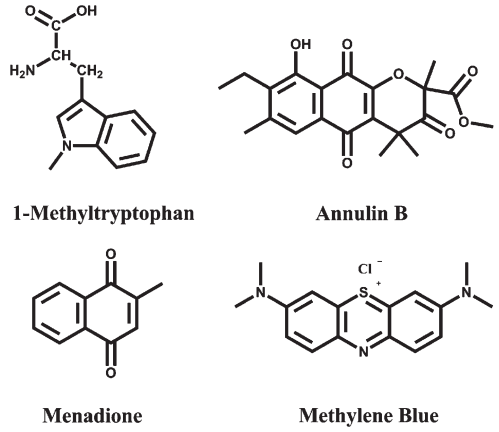

FIGURE 8: Relevant chemical structures. Structures of 1-methyltryptophan (1-MT), annulin B, menadione, and methylene blue.

concentrations of CPR of 0.87 ± 0.01 s^{-1} (Figure 1C). Due to the potential differences in the conformation of IDO when L-Trp is bound versus D-Trp (substrate inhibition kinetics versus Michaelis−Menten), the "effective" K_m value for oxidation of D-Trp may not accurately describe the interaction of CPR with IDO for L-Trp oxidation.

The addition of cytochrome b_5 to reconstitutions of recombinant CPR in lipids leads to an increase in catalytic rate for both L- and D-Trp, with D-Trp continuing to display Michaelis−Menten kinetics but L-Trp kinetics undergoing a cytochrome b_5 concentration-dependent change from substrate inhibition to sigmoidal. A plot of cytochrome b_5 concentration versus reaction velocity at saturating concentrations for both L- and D-Trp yields equivalent "effective" K_m values, arguing that in the presence of CPR the interaction of IDO with cytochrome b_5 is not altered by the stereochemistry of the tryptophan substrate. We are currently taking more direct approaches to measure the interactions between CPR/IDO and CPR/IDO/cytochrome b_5 in the presence of various ligands and substrates.

The results herein demonstrate that CPR with NADPH supports the biotransformation of tryptophan to *N*-formylkynurenine. These findings contradict previously reported data from Maghzal et al., where CPR alone did not support NADPH-dependent oxidation of tryptophan. This discrepancy could be explained by two differences in our assays. Foremost, in our hands the dilution of CPR without prior reconstitution into lipids resulted in undetectable formation of kynurenine over background. However, CPR premixed with cytochrome b_5 (without lipids) before dilution into IDO reaction mixes did show slight activity over background (data not shown). Second, the previous study assessed activity at a single concentration of L-Trp (400 μM). This concentration is approximately 45-fold above our K_i for the observed substrate inhibition kinetics with CPR as the cofactor. Therefore, under such conditions the activity may be markedly suppressed in the absence of cytochrome b_5.

The kinetic constants for ascorbate/methylene blue-supported oxidation reactions of L- and D-Trp are comparable to values reported in the literature with our K_m values being slightly higher affinity (for L-Trp a value of 3 vs 7.1−20 μM and for D-Trp 1 vs 2.6−5 mM) and our k_{cat} values slightly slower (for L-Trp a value of ~1 vs 2−5 s^{-1} and for D-Trp 1.7 vs 2.6−5.9 s^{-1}) (*39*, *46*, *47*). These differences may be attributed to differences in assay design (pH, buffering system, detection method, etc.). As reported previously (*37*, *39*), the ascorbate/methylene blue-supported oxidation of L-Trp displays substrate inhibition kinetics as

observed in our CPR system, but with an ~24-fold increase in K_i; i.e., in the presence of methylene blue the inhibitory substrate binding site has a lower affinity for the substrate L-Trp (Figure 3, Supporting Information Figure 1A). In parallel, D-Trp sees a similar decrease in affinity (~12−20-fold change in K_m) with the ascorbate/methylene blue reduction system compared to the CPR (±cytochrome b_5) system. These observations warranted further investigation into the potential role methylene blue plays in disrupting substrate binding. Addition of methylene blue (minus ascorbate) to CPR- (±cytochrome b_5) supported IDO incubations leads to altered kinetics for both isomers of Trp (Figures 4 and 5). For D-Trp, addition of methylene blue results in competitive inhibition for CPR-supported reactions which changes to mixed-mode inhibition in the presence of cytochrome b_5 (250 nM). Addition of methylene blue to CPR- (±cytochrome b_5) supported L-Trp oxidation reactions results in loss of the observed atypical kinetics (substrate inhibition for CPR and sigmoidal for CPR plus cytochrome b_5), yielding Michaelis−Menten kinetics. For both L- and D-Trp, addition of methylene blue to CPR-supported incubations (± cytochrome b_5) results in a concentration-dependent decrease in catalytic efficiency (Figure 5C) driven primarily by a decrease in affinity for the substrate.

The observed substrate inhibition kinetics for ascorbate/methylene blue-supported IDO oxidation of L-Trp is well established for concentrations of L-Trp above 50 μM (*37*, *39*). Lu et al. proposed that the observed substrate inhibition kinetics were due to binding of a second molecule of L-Trp to an inhibitory site, S_i, which becomes available upon binding of the first molecule of L-Trp (*39*). Nickel et al. in collaboration with Lu have recently shown by CO flash photolysis that CO rebinding is hindered by elevated concentrations of L-Trp (4.8 and 20 mM) (*48*). Based on this work and their ascorbate/methylene blue-supported kinetics, the authors propose that L-Trp binding at the S_i site leads to substrate inhibition through the inhibition of O_2 association (*39*, *48*).

In principle, partial substrate inhibition kinetics arise from allosteric interactions (*36*, *49*). Allosteric interactions can arise through ligand-induced conformational changes resulting from substrate or effector binding or through substrate/effector or substrate/substrate interactions within the active site (*35*, *50*, *51*). CPR-supported L-Trp oxidation steady-state kinetics display partial substrate inhibition which can be altered by the addition of cytochrome b_5, resulting in sigmoidal kinetics. The switch from substrate inhibition to sigmoidal kinetics leads to an increase in the rate of catalysis without loss of allosteric kinetics. This increase in catalytic rate upon the addition of cytochrome b_5, therefore, could result from cytochrome b_5/IDO protein interactions leading to rearrangement of the IDO active site making O_2 more accessible to the heme iron (as proposed by Nickel) or rearrangement of bound substrate into a more productive orientation above the catalytic iron.

In silico modeling was used to identify a potential effector molecule binding site. SiteMap has been successfully utilized to identify novel α sites (active sites) in proteins (*52*, *53*). The combination of SiteMap with the docking algorithm Glide was employed in an attempt to identify the potential allosteric site from an L-Trp-docked IDO structure (PDB entry 2D0T; 4-phenylimidazole-bound structure (*43*)). A site directly adjacent to heme was identified as the primary α site (active site) from this L-Trp-docked structure (Figure 7). Interestingly, the new site created from the docked model possessed similar hydrophobic surface area to that of the L-Trp binding pocket, suggesting the new α site may also be suitable for binding an additional small molecule. Moreover, the proximity of the secondary site is close enough to directly impact interactions at the active site, either through direct contact with the primary ligand or through indirect interaction with the heme or adjacent protein structure used to sequester the heme.

Whether the observed homotropic effects are due to substrate-induced conformational changes or ligand/ligand interactions within the active site requires further investigation. IDO is susceptible to allosteric modulation by substrates, electron transfer partners (cytochrome b_5), and small molecule effectors (*37*, *39*). As summarized by Lu, the development of more efficient IDO inhibitors will require further understanding of IDO enzymology and further characterization of the effector binding site. As shown here for menadione, incubation conditions can lead to differential inhibition.

Menadione effectively inhibits the oxidation of L-Trp using the chemical reductant system of ascorbate and methylene blue whereas menadione does not exhibit inhibition using the CPR (±cytochrome b_5) reduction system described herein. The mechanism for loss of inhibition is unclear; one proposal involves the possibility that menadione disrupts methylene blue binding and subsequent electron transfer to IDO but does not interfere with L-Trp binding such that total inhibitory activity by menadione is lost with the CPR reducing system. Other mechanisms are possible. Incubations with CPR ± b_5 require reconstitution of the coenzymes into lipids, which could potentially sequester the inhibitor menadione. One would expect, however, sequestration of menadione to result in a shift of the IC_{50} curve to the right due to a lower free fraction of menadione, not a complete loss of inhibition. Another possible explanation for the lack of inhibition by menadione in the CPR reducing system is the potential for menadione to be reduced by methylene blue. Reduction of menadione in the methylene blue/ascorbate system would disrupt electron transfer to IDO. We are currently investigating further the mechanism of menadione inhibition as menadione has been reported to inhibit IDO in a clonal T-REx-derived cell line stably transfected with doxycyclin-inducible IDO. Menadione, a known cytotoxic agent (*54*, *55*), exhibited an ~4-fold difference between inhibitory potency toward IDO (IC_{50} = 28.9 μM) and the measured LD_{50} for cellular cytotoxicity (128 μM) (*41*), but these data are difficult to interpret as cellular kynurenine levels were measured utilizing the nonspecific aldehyde and ketone reactive Ehrlich reagent (*p*-dimethylaminobenzaldehyde in strong acid medium) which has been shown to lack selectivity for kynurenine (*56*).

The potential for alternate electron transfer partners for IDO is a distinct possibility. Herein we present enzymatic activity from IDO when reconstituted with CPR. However, other active reductases, including NADH CoQ reductase (NOQ) and inducible nitric oxide synthase (iNOS), share similar properties and need to be investigated further as potential in vivo coenzymes of IDO. iNOS in particular is of interest, as it has been characterized as having a CPR-like domain (*57*), and iNOS and nitric oxide formation can impact IDO activity (*58*, *59*). Regardless of which reductase(s) is the actual in vivo cofactor to IDO, the idea of IDO allostery is an attractive one knowing its immunosuppressive role, where enzymatic activity can be tightly regulated by cofactors, effectors, or electron transfer partners and not by changes in endogenous tryptophan levels (50−100 μM in humans (*60*−*62*)). For example, the observed partial substrate

inhibition may function to maintain a basal level of IDO activity, where formation of kynurenine pathway metabolites is minimized. Subsequent changes in the gene expression of allosteric effectors, i.e., cytochrome b_5, could then lead to activation of IDO generating elevated levels of kynurenine and downstream metabolites that participate in immunosuppression (*63*−*66*).

CONCLUSION

The current study investigated whether CPR alone can support IDO enzymatic activity and whether the addition of additional electron transfer partners or cofactors used to support IDO activity such as cytochrome b_5 and methylene blue differentially impact IDO activity. The data presented demonstrate that CPR is capable of supporting IDO enzymatic activity and display differential kinetics for the two isomers of Trp, with the observed L-Trp partial substrate inhibition arguing for the binding of two substrate molecules. Addition of cytochrome b_5 to CPR-supported L-Trp incubations resulted in a switch from negative to positive homotropic cooperativity. Addition of methylene blue (minus ascorbate) to CPR-supported incubations also resulted in modulation of IDO enzymatic activity but differed from that of cytochrome b_5 in that it resulted in a decrease in catalytic efficiency for both L- and D-Trp oxidations driven by a decrease in affinity of IDO for both substrates. In conclusion, our data indicate that CPR is capable of supporting IDO activity in vitro and oxidation of tryptophan by IDO displays substrate stereochemistry dependent atypical kinetics which can be modulated by the addition of cytochrome b_5.

ACKNOWLEDGMENT

We are grateful to Dr. John J. Hill at Amgen Department of Protein Sciences for helpful discussions and critical review of the manuscript.

SUPPORTING INFORMATION AVAILABLE

Two tables presenting data on the changes in kinetic constants for L- and D-Trp oxidation by recombinant human IDO in the presence of CPR (Table 1) and CPR plus cytochrome b_5 (Table 2) with two figures presenting the UV−vis spectrum of our recombinant IDO preparation and a figure of the observed steady-state turnover rates for L- and D-Trp with ascorbate and methylene blue as the reducing system. This material is available free of charge via the Internet at http://pubs.acs.org.

REFERENCES

1. Yamamoto, S., and Hayaishi, O. (1967) Tryptophan pyrrolase of rabbit intestine. D- and L-tryptophan-cleaving enzyme or enzymes. *J. Biol. Chem. 242*, 5260–5266.
2. Higuchi, K., and Hayaishi, O. (1967) Enzymic formation of D-kynurenine from D-tryptophan. *Arch. Biochem. Biophys. 120*, 397–403.
3. Hirata, F., and Hayaishi, O. (1972) New degradative routes of 5-hydroxytryptophan and serotonin by intestinal tryptophan 2,3-dioxygenase. *Biochem. Biophys. Res. Commun. 47*, 1112–1119.
4. Moffett, J. R., and Namboodiri, M. A. (2003) Tryptophan and the immune response. *Immunol. Cell Biol. 81*, 247–265.
5. Mellor, A. L., and Munn, D. H. (2004) IDO expression by dendritic cells: tolerance and tryptophan catabolism. *Nat. Rev. 4*, 762–774.
6. Beutelspacher, S. C. (2006) Expression of indoleamine 2,3-dioxygenase (IDO) by endothelial cells: implications for the control of alloresponses. *Am. J. Transplant. 6*, 1320–1330.
7. Munn, D. H. (2004) Expression of indoleamine 2,3-dioxygenase by plasmacytoid dendritic cells in tumor-draining lymph nodes. *J. Clin. Invest. 114*, 280–290.
8. Uyttenhove, C. (2003) Evidence for a tumoral immune resistance mechanism based on tryptophan degradation by indoleamine 2,3-dioxygenase. *Nat. Med. 9*, 1269–1274.
9. Orabona, C., Puccetti, P., Vacca, C., Bicciato, S., Luchini, A., Fallarino, F., Bianchi, R., Velardi, E., Perruccio, K., Velardi, A., Bronte, V., Fioretti, M. C., and Grohmann, U. (2006) Toward the identification of a tolerogenic signature in IDO-competent dendritic cells. *Blood 107*, 2846–2854.
10. Odemuyiwa, S. O., Ghahary, A., Li, Y., Puttagunta, L., Lee, J. E., Musat-Marcu, S., Ghahary, A., and Moqbel, R. (2004) Cutting edge: human eosinophils regulate T cell subset selection through indoleamine 2,3-dioxygenase. *J. Immunol. 173*, 5909–5913.
11. Yoshida, R., Imanishi, J., Oku, T., Kishida, T., and Hayaishi, O. (1981) Induction of pulmonary indoleamine 2,3-dioxygenase by interferon. *Proc. Natl. Acad. Sci. U.S.A. 78*, 129–132.
12. Pfefferkorn, E. R. (1984) Interferon gamma blocks the growth of *Toxoplasma gondii* in human fibroblasts by inducing the host cells to degrade tryptophan. *Proc. Natl. Acad. Sci. U.S.A. 81*, 908–912.
13. Munn, D. H. (1998) Prevention of allogeneic fetal rejection by tryptophan catabolism. *Science 281*, 1191–1193.
14. Grohmann, U. (2002) CTLA-4-Ig regulates tryptophan catabolism in vivo. *Nat. Immunol. 3*, 1097–1101.
15. Swanson, K. A., Zheng, Y., Heidler, K. M., Mizobuchi, T., and Wilkes, D. S. (2004) CDllc+ cells modulate pulmonary immune responses by production of indoleamine 2,3-dioxygenase. *Am. J. Resp. Cell Mol. Biol. 30*, 311–318.
16. Gurtner, G. J., Newberry, R. D., Schloemann, S. R., McDonald, K. G., and Stenson, W. F. (2003) Inhibition of indoleamine 2,3-dioxygenase augments trinitrobenzene sulfonic acid colitis in mice. *Gastroenterology 125*, 1762–1773.
17. Hayashi, T., Beck, L., Rossetto, C., Gong, X., Takikawa, O., Takabayashi, K., Broide, D. H., Carson, D. A., and Raz, E. (2004) Inhibition of experimental asthma by indoleamine 2,3-dioxygenase. *J. Clin. Invest. 114*, 270–279.
18. Kwidzinski, E., Bunse, J., Aktas, O., Richter, D., Mutlu, L., Zipp, F., Nitsch, R., and Bechmann, I. (2005) Indolamine 2,3-dioxygenase is expressed in the CNS and down-regulates autoimmune inflammation. *FASEB J. 19*, 1347–1349.
19. Brandacher, G. (2006) Prognostic value of indoleamine 2,3-dioxygenase expression in colorectal cancer: effect on tumor-infiltrating T cells. *Clin. Cancer Res. 12*, 1144–1151.
20. Okamoto, A., Nikaido, T., Ochiai, K., Takakura, S., Saito, M., Aoki, Y., Ishii, N., Yanaihara, N., Yamada, K., Takikawa, O., Kawaguchi, R., Isonishi, S., Tanaka, T., and Urashima, M. (2005) Indoleamine 2,3-dioxygenase serves as a marker of poor prognosis in gene expression profiles of serous ovarian cancer cells. *Clin. Cancer Res. 11*, 6030–6039.
21. Yamazaki, H., Nakano, M., Imai, Y., Ueng, Y. F., Guengerich, F. P., and Shimada, T. (1996) Roles of cytochrome b_5 in the oxidation of testosterone and nifedipine by recombinant cytochrome P450 3A4 and by human liver microsomes. *Arch. Biochem. Biophys. 325*, 174–182.
22. Bell, L. C., and Guengerich, F. P. (1997) Oxidation kinetics of ethanol by human cytochrome P450 2E1. Rate-limiting product release accounts for effects of isotopic hydrogen substitution and cytochrome b_5 on steady-state kinetics. *J. Biol. Chem. 272*, 29643–29651.
23. Perret, A., and Pompon, D. (1998) Electron shuttle between membrane-bound cytochrome P450 3A4 and b_5 rules uncoupling mechanisms. *Biochemistry 37*, 11412–11424.
24. Reedy, C. J., Elvekrog, M. M., and Gibney, B. R. (2008) Development of a heme protein structure-electrochemical function database. *Nucleic Acids Res. 36*, D307–D313.
25. Maghzal, G. J., Thomas, S. R., Hunt, N. H., and Stocker, R. (2008) Cytochrome b_5, not superoxide anion radical, is a major reductant of indoleamine 2,3-dioxygenase in human cells. *J. Biol. Chem. 283*, 12014–12025.
26. Vottero, E., Mitchell, D. A., Page, M. J., MacGillivray, R. T., Sadowski, I. J., Roberge, M., and Mauk, A. G. (2006) Cytochrome b(5) is a major reductant in vivo of human indoleamine 2,3-dioxygenase expressed in yeast. *FEBS Lett. 580*, 2265–2268.
27. Paine, M. J. I. (2005) Electron Transfer Partners of Cytochrome P450, in Cytochrome P450: Structure, Mechanism, and Biochemistry (Ortiz de Montellano, P. R., Ed.) 3rd ed., pp 115−148, Kluwer Academic Publishers, New York.
28. Schenkman, J. B., Voznesensky, A. I., and Jansson, I. (1994) Influence of ionic strength on the P450 monooxygenase reaction and role of cytochrome b_5 in the process. *Arch. Biochem. Biophys. 314*, 234–241.
29. Yamazaki, H., Johnson, W. W., Ueng, Y. F., Shimada, T., and Guengerich, F. P. (1996) Lack of electron transfer from cytochrome b_5 in stimulation of catalytic activities of cytochrome P450 3A4. Characterization of a reconstituted cytochrome P450 3A4/NADPH-cytochrome

P450 reductase system and studies with apo-cytochrome b_5. *J. Biol. Chem. 271*, 27438–27444.
30. Yamazaki, H., Shimada, T., Martin, M. V., and Guengerich, F. P. (2001) Stimulation of cytochrome P450 reactions by apo-cytochrome b_5: evidence against transfer of heme from cytochrome P450 3A4 to apo-cytochrome b_5 or heme oxygenase. *J. Biol. Chem. 276*, 30885–30891.
31. Gruenke, L. D., Konopka, K., Cadieu, M., and Waskell, L. (1995) The stoichiometry of the cytochrome P-450-catalyzed metabolism of methoxyflurane and benzphetamine in the presence and absence of cytochrome b_5. *J. Biol. Chem. 270*, 24707–24718.
32. Korzekwa, K. R., Krishnamachary, N., Shou, M., Ogai, A., Parise, R. A., Rettie, A. E., Gonzalez, F. J., and Tracy, T. S. (1998) Evaluation of atypical cytochrome P450 kinetics with two-substrate models: evidence that multiple substrates can simultaneously bind to cytochrome P450 active sites. *Biochemistry 37*, 4137–4147.
33. Shou, M., Dai, R., Cui, D., Korzekwa, K. R., Baillie, T. A., and Rushmore, T. H. (2001) A kinetic model for the metabolic interaction of two substrates at the active site of cytochrome P450 3A4. *J. Biol. Chem. 276*, 2256–2262.
34. Wang, R. W., Newton, D. J., Liu, N., Atkins, W. M., and Lu, A. Y. (2000) Human cytochrome P-450 3A4: in vitro drug-drug interaction patterns are substrate-dependent. *Drug Metab. Dispos. 28*, 360–366.
35. Dabrowski, M. J., Schrag, M. L., Wienkers, L. C., and Atkins, W. M. (2002) Pyrene·pyrene complexes at the active site of cytochrome P450 3A4: evidence for a multiple substrate binding site. *J. Am. Chem. Soc. 124*, 11866–11867.
36. Atkins, W. M., Wang, R. W., and Lu, A. Y. (2001) Allosteric behavior in cytochrome p450-dependent in vitro drug-drug interactions: a prospective based on conformational dynamics. *Chem. Res. Toxicol. 14*, 338–347.
37. Sono, M. (1989) Enzyme kinetic and spectroscopic studies of inhibitor and effector interactions with indoleamine 2,3-dioxygenase. 2. Evidence for the existence of another binding site in the enzyme for indole derivative effectors. *Biochemistry 28*, 5400–5407.
38. Sono, M., Taniguchi, T., Watanabe, Y., and Hayaishi, O. (1980) Indoleamine 2,3-dioxygenase. Equilibrium studies of the tryptophan binding to the ferric, ferrous, and CO-bound enzymes. *J. Biol. Chem. 255*, 1339–1345.
39. Lu, C., Lin, Y., and Yeh, S. R. (2009) Inhibitory substrate binding site of human indoleamine 2,3-dioxygenase. *J. Am. Chem. Soc. 131*, 12866–12867.
40. Shaw, P. M., Hosea, N. A., Thompson, D. V., Lenius, J. M., and Guengerich, F. P. (1997) Reconstitution premixes for assays using purified recombinant human cytochrome P450, NADPH-cytochrome P450 reductase, and cytochrome b_5. *Arch. Biochem. Biophys. 348*, 107–115.
41. Kumar, S. (2008) Structure based development of phenylimidazole-derived inhibitors of indoleamine 2,3-dioxygenase. *J. Med. Chem. 51*, 4968–4977.
42. Shou, M. (2002) Kinetic analysis for multiple substrate interaction at the active site of cytochrome P450. *Methods Enzymol. 357*, 261–276.
43. Sugimoto, H. (2006) Crystal structure of human indoleamine 2,3-dioxygenase: catalytic mechanism of O2 incorporation by a heme-containing dioxygenase. *Proc. Natl. Acad. Sci. U.S.A. 103*, 2611–2616.
44. Houston, J. B. (2003) Typical and Atypical Enzyme Kinetics, in Drug Metabolizing Enzymes: Cytochrome P450 and Other Enzymes in Drug Discovery and Development (Jae, S., Lee, R. S. O., and Fischer, M. B., Eds.) pp 211−251, CRC PressBoca Raton, FL.
45. Pereira, A., Vottero, E., Roberge, M., Mauk, A. G., and Andersen, R. J. (2006) Indoleamine 2,3-dioxygenase inhibitors from the Northeastern Pacific marine hydroid *Garveia annulata*. *J. Nat. Prod. 69*, 1496–1499.
46. Littlejohn, T. K., Takikawa, O., Truscott, R. J., and Walker, M. J. (2003) Asp274 and his346 are essential for heme binding and catalytic function of human indoleamine 2,3-dioxygenase. *J. Biol. Chem. 278*, 29525–29531.
47. Papadopoulou, N. D., Mewies, M., McLean, K. J., Seward, H. E., Svistunenko, D. A., Munro, A. W., and Raven, E. L. (2005) Redox and spectroscopic properties of human indoleamine 2,3-dioxygenase and a His303Ala variant: implications for catalysis. *Biochemistry 44*, 14318–14328.
48. Nickel, E., Nienhaus, K., Lu, C., Yeh, S. R., Nienhaus, G. U. (2009) Ligand and substrate migration in human indoleamine 2,3-dioxygenase, J. Biol. Chem. (in press).
49. Atkins, W. M. (2005) Non-Michaelis-Menten kinetics in cytochrome P450-catalyzed reactions. *Annu. Rev. Pharmacol. Toxicol. 45*, 291–310.
50. Davydov, D. R., Davydova, N. Y., Tsalkova, T. N., and Halpert, J. R. (2008) Effect of glutathione on homo- and heterotropic cooperativity in cytochrome P450 3A4. *Arch. Biochem. Biophys. 471*, 134–145.
51. Davydov, D. R., and Halpert, J. R. (2008) Allosteric P450 mechanisms: multiple binding sites, multiple conformers or both? *Expert Opin. Drug Metab. Toxicol. 4*, 1523–1535.
52. Halgren, T. (2007) New method for fast and accurate binding-site identification and analysis. *Chem. Biol. Drug Des. 69*, 146–148.
53. Halgren, T. A. (2009) Identifying and characterizing binding sites and assessing druggability. *J. Chem. Inf. Modeling 49*, 377–389.
54. McAmis, W. C., Schaeffer, R. C., Jr., Baynes, J. W., and Wolf, M. B. (2003) Menadione causes endothelial barrier failure by a direct effect on intracellular thiols, independent of reactive oxidant production. *Biochim. Biophys. Acta 1641*, 43–53.
55. Ross, D., Thor, H., Orrenius, S., and Moldeus, P. (1985) Interaction of menadione (2-methyl-1,4-naphthoquinone) with glutathione. *Chem.−Biol. Interact. 55*, 177–184.
56. Alegre, E., Lopez, A. S., and Gonzalez, A. (2005) Tryptophan metabolites interfere with the Ehrlich reaction used for the measurement of kynurenine. *Anal. Biochem. 339*, 188–189.
57. Yamamoto, K., Kimura, S., Shiro, Y., and Iyanagi, T. (2005) Interflavin one-electron transfer in the inducible nitric oxide synthase reductase domain and NADPH-cytochrome P450 reductase. *Arch. Biochem. Biophys. 440*, 65–78.
58. Samelson-Jones, B. J., and Yeh, S. R. (2006) Interactions between nitric oxide and indoleamine 2,3-dioxygenase. *Biochemistry 45*, 8527–8538.
59. Thomas, S. R., Mohr, D., and Stocker, R. (1994) Nitric oxide inhibits indoleamine 2,3-dioxygenase activity in interferon-gamma primed mononuclear phagocytes. *J. Biol. Chem. 269*, 14457–14464.
60. Amirkhani, A., Heldin, E., Markides, K. E., and Bergquist, J. (2002) Quantitation of tryptophan, kynurenine and kynurenic acid in human plasma by capillary liquid chromatography-electrospray ionization tandem mass spectrometry. *J. Chromatogr. 780*, 381–387.
61. Huengsberg, M., Winer, J. B., Gompels, M., Round, R., Ross, J., and Shahmanesh, M. (1998) Serum kynurenine-to-tryptophan ratio increases with progressive disease in HIV-infected patients. *Clin. Chem. 44*, 858–862.
62. Laich, A., Neurauter, G., Widner, B., and Fuchs, D. (2002) More rapid method for simultaneous measurement of tryptophan and kynurenine by HPLC. *Clin. Chem. 48*, 579–581.
63. Fallarino, F. (2003) T cell apoptosis by kynurenines. *Adv. Exp. Med. Biol. 527*, 183–190.
64. Frumento, G. (2002) Tryptophan-derived catabolites are responsible for inhibition of T and natural killer cell proliferation induced by indoleamine 2,3-dioxygenase. *J. Exp. Med. 196*, 459–468.
65. Terness, P. (2002) Inhibition of allogeneic T cell proliferation by indoleamine 2,3-dioxygenase-expressing dendritic cells: mediation of suppression by tryptophan metabolites. *J. Exp. Med. 196*, 447–457.
66. Chen, W., Liang, X., Peterson, A. J., Munn, D. H., and Blazar, B. R. (2008) The indoleamine 2,3-dioxygenase pathway is essential for human plasmacytoid dendritic cell-induced adaptive T regulatory cell generation. *J. Immunol. 181*, 5396–5404.